Chaos in Magnetoplasmas

B. Buti

Nonlinear Processes in Geophysics (1999) 6: 129–143

Nonlinear Processes in Geophysics

Chaos in magnetoplasmas

B. Buti

Jet Propulsion Laboratory, California Institute of Technology, Pasadena, CA 91109, USA

Received: 7 June 1999 – Revised: 25 August 1999 – Accepted: 8 October 1999

Abstract. A nonlinear wave, in general, is equivalent to a nonlinear dynamical system, which exhibits the phenomena of chaos. By means of techniques of nonlinear dynamical systems, we have investigated the conditions under which nonlinear Alfvén waves and lower-hybrid waves can become chaotic. The role of heavy ions, in controlling the chaos in magnetoplasmas, is examined. Chaotic routes to Alfvénic turbulence, with k^{-1} spectra, are observed in case of externally driven nonlinear Alfvén waves. Anomalous heating and particle acceleration resulting from chaotic fields, generated by lower-hybrid waves, are briefly outlined.

1 Introduction

The subject, of Chaos, is truly interdisciplinary. It occurs in a variety of physical Systems e.g., astrophysics, geophysics, optics, condensed matter physics, plasmas, fluids etc. and also in chemical systems, atmospheric sciences, biophysics, neural networks etc. The mathematical techniques, to study chaotic phenomena in any of these systems, are the techniques of nonlinear dynamics. Historically Jules - Henry Poincare was the first person to recognize the chaotic behaviour of a dynamical system. He encountered this unexpected behaviour in his studies of three-body problems in planetary systems. The puzzeling behaviour encountered by Poincare was simply because he was dealing with nonintegrable systems, which are defined as : A system with N degrees of freedom, if it has N independent integrals of motion, is an integrable system. This is only a necessary condition for integrability. The necessary and sufficient condition for integrability is satisfied only if N independent constants of motion $C_1, C_2, C_3, ...C_N$ are in involution i.e., $\{C_i, C_j\} = 0$, where $\{\ \}$ represents the Poisson Bracket. An integrable system, e.g., systems governed by nonlinear evolution equations like KdV, Nonlinear Schrödinger (NLS) and Derivative Nonlinear Schrödinger (DNLS), can never lead to chaos whereas a nonintegrable system could. As a beautiful, simple example of a nonitegrable plasma system, we can mention the motion of a charged particle in a magnetic field of the form: $\mathbf{B} = \hat{e}_x\, B_0\, tanh(z/\delta) + \hat{e}_z\, B_n$. This field characterizes the quasi neutral sheet of thickness δ. B_n, the normal component of the magnetic field, no matter how small, leads to stochasticity in the otherwise integrable system (Buti, 1988).This happens since the system loses the involution property due to the presence of B_n. Chaos also appears when perturbations are applied to integrable systems (Contopoulos, 1985).

The study of phenomena of chaos, in plasmas, is being pursued essentially to understand the phenomena of plasma turbulence which is very often observed in laboratory, space as well as in astrophysical plasmas (cf. Ashour-Abdalla and Baker, 1991 and other papers in this special issue on Chaos and Stochasticity in Space Plasmas). Alfvén waves are a ubiquitous feature of magnetoplasmas. Implications of existence of large-amplitude Alfvén waves in many cosmic plasmas have been investigated. Some of these examples include turbulent heating of stellar corona (Pettini et al., 1985), coherent radio emissions (Lakhina and Buti, 1988; Lakhina, Buti and Tsinsadze, 1990), interstellar scintillations of radio sources (Spangler, 1991), generation of stellar winds and extragalactic jets (Jatenco-Pereira, 1995) etc. Alfvén wave trains as well as Alfvénic turbulence have long been observed in the solar wind (Belcher and Davis, 1971) and cometary plasmas (Scarf et al., 1986; Tsurutani and Smith, 1986). Burlaga (1991a, 1991b and references therein) has done the detailed analysis of the solar wind data obtained from various space crafts; he found some signatures of chaos e.g., multifractals and intermittent turbulence in the solar wind. Observations of Alfvénic intermittent turbulence are also reported by Marsch and Liu (1993) and Tu and Marsch (1995). All these observations are clear indications of the significance of investigating the nonlinear and chaotic behaviour of Alfvén waves. Some theoretical attempts (Ghosh and Papadopoulos, 1987; Hada et al., 1990; Buti, 1992; 1997; 1998; Buti

Correspondence to: B. Buti

and Nocera, 1999a; Nocera and Buti, 1996; 1998) have been made to study these chaotic Alfvén waves. Hada et al. (1990) had included dissipative effects whereas kinetic effects were incorporated into the DNLS equation by Rogister (1971), Mjolhus and Wyller (1986, 1988), Spangler (1989, 1990) and Medvedev and Diamond (1996).

Besides Alfvén waves, lower - hybrid waves are also observed in a variety of plasmas. It is known that these waves can become unstable due to a variety of free energy sources. The conditions under which lower-hybrid waves become chaotic have been investigated by Smith and Kaufman (1975), Karney and Bers (1977) and Karney (1978) . The problem of anomalous acceleration, of heavy ions by chaotic lower-hybrid waves in the cometary environment, has been studied by Buti and lakhina (1987). In solar corona also the lower - hybrid waves can be excited when the hot (nonthermal) electron beams, escaping the injection region (top of the coronal loop) along the coronal magnetic field lines, impinge on the cooler chromospheric plasma at the foot of the coronal loop. Lakhina and Buti (1996), found that the chaotic lower - hybrid waves can provide a potential source for the anomalous acceleration in the solar corona. The present paper is essentially an overview of the chaotic Alfvén and lower-hybrid waves .

2 CHAOTIC ALFVÉN WAVES

The governing equations for finite-amplitude Alfvén Waves in a dispersive medium, like a magneto-plasma, are the dispersive MHD equations:

$$\frac{\partial \rho}{\partial t} + \nabla \cdot (\rho \mathbf{v}) = 0, \tag{1a}$$

$$\rho \frac{d\mathbf{v}}{dt} = -\nabla p + \mathbf{J} \times \mathbf{B}, \tag{1b}$$

and

$$\frac{\partial \mathbf{B}}{\partial t} = \nabla \times \left[(\mathbf{v} \times \mathbf{B}) - \frac{1}{\rho} (\nabla \times \mathbf{B}) \times \mathbf{B} \right] \tag{1c}$$

In eq.(1), $\mathbf{B}$ is normalized to B_0, $\mathbf{v}$ to $V_A = B_0/(4\pi\rho_0)^{1/2}$ (V_A being the speed of Alfvén Waves), ρ to ρ_0, t to inverse of Ω_i, the ion cyclotron frequency and l to V_A/Ω_i. The subscript '0' refers to the equilibrium quantities. Note that the second term on the right hand side of Eq.(1c) is due to ion inertial effects in the generalized Ohms law. We would like to point out that the set of equations (1) would not be valid for systems with $\beta \sim 1$ because in that case the kinetic effects become important.

2.1 Evolution Equation for Alfvén Waves in Homogeneous Plasma

For wave propagation along the direction of a uniform magnetic field i.e., along x - axis, Eqs.(1) simplify to :

$$\frac{\partial \rho}{\partial t} + \frac{\partial}{\partial x}(\rho v_x) = 0, \tag{2}$$

$$\frac{\partial}{\partial t}(\rho v_x) + \frac{\partial}{\partial x}(\rho {v_x}^2) + \frac{\partial \beta}{\partial x} + \frac{\partial}{\partial x}\left(\frac{B^2}{2}\right) = 0, \tag{3}$$

$$\frac{\partial}{\partial t}(\rho \tilde{v}) + \frac{\partial}{\partial x}(\rho v_x \tilde{v}) - \frac{\partial B}{\partial x} = 0, \tag{4}$$

$$\frac{\partial B}{\partial t} + \frac{\partial}{\partial x}(v_x B - \tilde{v}) = -i \frac{\partial}{\partial x}\left(\frac{1}{\rho}\frac{\partial B}{\partial x}\right), \tag{5}$$

and

$$\frac{\partial \beta}{\partial t} + \frac{\partial}{\partial x}(\beta v_x) + (\gamma - 1)\beta \frac{\partial v_x}{\partial x} = 0, \tag{6}$$

where v_x is the flow velocity along the direction of propagation, γ is the ratio of the specific heat, $B = (B_y + i\, B_z)$ and $\tilde{v} = (v_y + i\, v_z)$. For pressure, we have used the adiabatic equation of state i.e., $p\rho^{-\gamma} = const.$

For $\beta \neq 1$, these equations have been simplified by using reductive perturbation methods (Tanuiti and Wei, 1968; Verheest and Buti, 1992; Buti, 1992; 1997). For the magnetic fluctuations carried to third order, they yield the following evolution equation:

$$\frac{\partial B_\pm}{\partial t} + \frac{1}{4\,(1-\beta)} \frac{\partial}{\partial x} \left(B_\pm \mid B_\pm \mid^2 \right) \pm \frac{i}{2} \frac{\partial^2 B_\pm}{\partial x^2} = 0. \tag{7}$$

Equation (7) is the well known derivative nonlinear Schrödinger (DNLS) equation. The plus and minus signs in the last term correspond to left ($B_+ = B$) and right hand (with $B_- = B_y - i\, B_z$) polarization respectively. Equation (7) is an integrable equation; one of its exact solution is given by (Kaup and Newell, 1978; Verheest and Buti, 1992):

$$B_\pm\,(x,\,t) \;=\; \frac{(2^{1/2}-1)^{1/2}\; B_s\; e^{\pm i\theta\,(\zeta)}}{[2^{1/2}\,\cosh\,(2\;V_s\;\zeta)\;-\;1]^{1/2}}, \tag{8}$$

where B_s is the amplitude of the soliton, $\zeta = (x - V_s t)$,

$$\theta\,(x,t) \;=\; -\,V_s\;\zeta + 3\;\tan^{-1}\,[(2^{1/2}+1)\;\tanh(2V_s\;\zeta)]. \tag{9}$$

θ is the phase and V_s is the soliton speed defined by,

$$V_s \;=\; \frac{(2^{1/2}-1)\;B_s^2}{8\;\mid(1\;-\;\beta)\mid}. \tag{10}$$

Hada et al. (1989) had shown that Eq.(7) can give a variety of solutions, namely, (1) periodic envelope modulations; (2) monochromatic waves; (3) hyperbolic solitons; (4) algebraic solitons. On using the Lagrangian approach, Kennel et al. (1988) had derived the vector derivative nonlinear Schrödinger (VDNLS) equation that governs elliptically polarized Alfvén Waves.

2.2 Evolution Equation for Alfvén Waves in Inhomogeneous Plasma

For Alfvén waves in inhomogeneous plasmas, once again by using the reductive perturbation method, Buti (1991, 1992a) had rederived the governing evolution equation. In this derivation, even though no explicit assumption about the homogeneity of the magnetic field was made, implicitly the magnetic field considered turned out to be homogeneous because of the following reason. The condition $div\ \mathbf{B}_0 = 0$, in slab geometry (with $k_y = k_z = 0$) demands that $\partial B_0/\partial x = 0$ i.e., ambient magnetic field be uniform. To overcome the restrictions imposed by this implicit assumption, Buti et al. (1999a) have incorporated spherical geometry. On using equations (1) in spherical co-ordinates and assuming no variations along θ and ϕ directions i.e., $\partial/\partial\theta = \partial/\partial\phi = 0$, Eqs. (1) reduce to:

$$\frac{\partial \rho}{\partial t} + \frac{1}{r^2}\frac{\partial}{\partial r}(r^2 \rho v_r) = 0, \tag{11a}$$

$$\rho \frac{dv_r}{dt} = -\frac{\partial p}{\partial r} - \frac{\partial}{\partial r}\frac{B_\perp^2}{2} - \frac{B_\perp^2}{2}, \tag{11b}$$

$$\rho \frac{d\mathbf{v}_\perp}{dt} = \frac{B_r}{r}\frac{\partial}{\partial r}(r\mathbf{B}_\perp), \tag{11c}$$

and

$$\frac{\partial \mathbf{B}_\perp}{\partial t} = \frac{1}{r}\frac{\partial}{\partial r}(B_r v_\perp - v_r B_\perp) + \frac{1}{r}\frac{\partial}{\partial r}\left[\frac{B\hat{\mathbf{e}}_r}{r\rho} \times \frac{\partial(\mathbf{B}_\perp r)}{\partial r}\right], \tag{11d}$$

where r is the radial distance, $\mathbf{B}_\perp = (B_\theta, B_\phi)$, $\mathbf{v}_\perp = (v_\theta, v_\phi)$, and $B_\perp^2 = (B_\theta^2 + B_\phi^2)$. Once again, for pressure, we use the adiabatic equation of state i.e., $p\rho^{-\gamma} = const.$ In order to satisfy eq.(11a) and the condition, $div\ \mathbf{B}_0 = 0$, the equilibrium density $\rho_0(r)$ and the magnetic field $B_0(r)$ must satisfy the conditions:

$$B_0(r)\ r^2 = const \tag{12}$$

and

$$\rho_0(r)\ U(r)\ r^2 = const. \tag{13}$$

For weakly nonlinear systems, we can use reductive perturbation scheme to derive the evolution equation from Eqs.(11). Following the procedure outlined in Buti (1991), we use the following stretchings:

$$\eta = \epsilon^2 r; \quad \xi = \epsilon\left[\int \frac{dr}{V(r)} - t\right] \tag{14}$$

In Eq.(14) ϵ is the stretching parameter and $V(r)$ is the phase velocity of the Alfvén wave that is given by

$$V(r) = U(r) + \frac{B_0(r)}{\rho_0^{1/2}(r)}. \tag{15}$$

In Eq.(15), U is the equilibrium streaming plasma velocity.

On using the expansions for density, velocity, pressure and magnetic field appropriate to Alfvén Waves (cf. Buti, 1991) for a spherically symmetric system, we obtain the following evolution (MDNLS) equation:

$$\frac{\partial B}{\partial \eta} + \frac{3\,U}{2\,V\,\eta}B + \frac{B}{4\,V\,(V-U)}\frac{\partial}{\partial \eta}(V^2 - U^2) + \frac{(V-U)}{4\,B_0^2(\eta)\,V^2\,(1-\beta(\eta))}\frac{\partial}{\partial \xi}(B \mid B \mid^2) + \frac{i\,(V-U)^2}{2\,V^3\,B_0(\eta)}\frac{\partial^2 B}{\partial \xi^2} = 0, \tag{16}$$

where $B = (B_\theta + i\,B_\phi)$, $\beta(\eta)$ is the plasma β, and $B_0(\eta)$ is the ambient magnetic field. In deriving Eq. (16), we have taken wave propagation as well as the ambient magnetic field along the radial direction. As in the case of the DNLS, here also we have neglected fifth order nonlinear terms. This equation, however, is valid for weak but arbitrary inhomogeneities. By weak we mean that the scale lengths of inhomogeneities be larger than the the widths of the DNLS solitons. This however is not equivalent to the WKB approximation; the latter is incompatible with the studies of turbulence that involve a variety of different scales. It was shown by Buti (1991) that extremely weak inhomogeneities, like the ones that could be treated by the WKB theory, affect only the amplitude of the soliton. The soliton acceleration and the consequent emission of radiations and also the turbulence (see Figs.1 and 2) can not be expected from Alfvénic systems whose evolution is based on the WKB approximation. We may note that for nonstreaming uniform plasmas i.e., for $U = 0$ and $\rho_0(r) = 1$, $V \to 1$ and Eq. (16) reduces to Eq.(7). It is worth noting that the roles of spatial and temporal variables are interchanged in Eq.(16). It is interesting to observe that this modified DNLS (Eq (16)), besides having additional two linear terms in B, has variable co-efficients for nonlinear and dispersive terms. Because of these complicated variable co-efficients, it is not possible to find an analytical solution to Eq. (16) and one has to look for its numerical solution.

Equation (16) has been solved numerically (Buti et al., 1999a) by means of the spectral collocation method. For the sake of computational convenience, we rewrite this equation as,

$$\frac{\partial B}{\partial \eta} + f(\eta)B + \alpha_1(\eta)\frac{\partial}{\partial \xi}(|B|^2 B) + i\alpha_2(\eta)\frac{\partial^2 B}{\partial \xi^2} = 0. \tag{17}$$

Since eq. (17) has temporal and spatial variables interchanged, we write the approximate solution for B as a Fourier expansion in time instead of space, namely

$$B(\xi,\eta) = \sum_{k=-N}^{N-1} b_k(\eta) e^{-i\lambda_k \xi}. \quad (18)$$

Note that B is assumed to be periodic in time, with period T and frequency $\lambda_k = 2\pi k/T$. For the numerical solution of the MDNLS, we do not need to introduce any artificial dissipation . In our case, inhomogeneous terms formally play the role of effective dissipation. As mentioned earlier, the problem of wave propagation is solved as an evolutionary problem in space. For this purpose, we assume that there is an influx of waves at one end of the interval (e.g., closer to the Sun in case of the solar wind plasma) and the waves are propagating outward. The influx is assumed periodic in time.

For the numerical solution, we have considered the evolution of an initial Alfvén soliton which is an exact solution of the DNLS equation and is given by,

$$B\,(\xi,\ r_0) \ = \ \frac{B_{max}\ e^{i\theta\,(\xi)}}{cosh^{1/2}\psi}, \quad (19)$$

with

$$\psi \ = \ (\xi \ - \ L/2)\ B_{max}^2\ /(\ 2\ \delta), \quad (20)$$

$$\theta\ (\xi) \ = \ \frac{3}{2}\ tan^{-1}\ (sinh\ \psi) \quad (21)$$

and

$$\delta \ = \ \frac{2}{V}\ (1 \ - \ \beta)\ (V \ - \ U). \quad (22)$$

B_{max} in Eq.(19) is the amplitude of the initial soliton normalized to $B_0\ (r_0)$ and L is the simulation box length. We would like to point out that the solution given in Eq.(19) is different than the one given by Eq.(8). In the soliton solution (Mjolhus, 1978) of the DNLS equation, there are two arbitrary constants κ_0 and ν_0. For Eq.(8), we had taken $\nu_0 = 0$ and now for Eq.(19) κ_0 has been taken to be zero.

The time evolution of the DNLS soliton at different spatial distances, from the reference point r_0, is shown in Fig.1. For the case of Alfvén waves propagating away from the sun in the interplanetary medium, this reference point could be $R_0 = 0.1AU$. From this figure, we clearly see the dissipative effects of the inhomogeneities. The amplitude of the soliton goes down as it propagates. Similar dissipative effects of inhomogeneities, in connection with modulated ion-acoustic waves, were reported by Mohan and Buti (1979). We also see the steepening of the wave and the high-frequency radiation on the leading edges. MHD simulations (see sec.5) also show similar behaviour. The frequency spectra for the magnetic field intensites are shown in Fig.2. The spectral index, for the power-law spectra, is increasing with the heliocentric distance. We also see breaks in the spectra. The break-point moves to the lower frequencies with the increasing distances

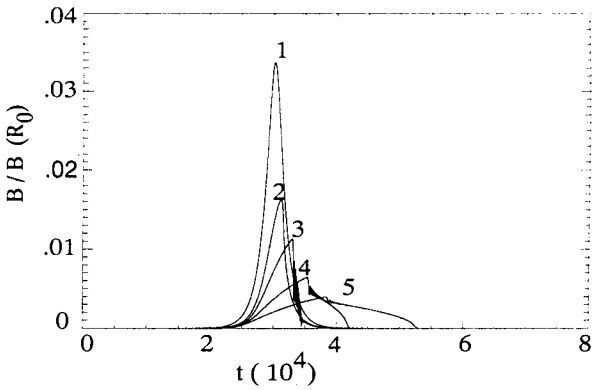

Fig. 1. Shows the evolution of $B\ /\ B_0(r_0)$ with t for $B_{max}\ (R_0)$ = 0.036, R_0 = 0.1 AU, U_0 = 1.5 V_{A0} and $\beta\ (R_0)\ =\ 0.05$. Curves labelled 1, 2, 3, 4 and 5 correspond to r = 0.1 AU, 0.35 AU, 0.5 AU, 0.7 AU and 0.9 AU. (from Buti et al., 1999a)

from the sun. Similar features have been observed in the turbulent solar wind spectra (Belcher and Davis, 1971; Bavassano et al., 1982) by Mariner 5 and Helios 1 and 2. Buti et al. (1999a) had looked into the evolution of initial circulatly polarized Alfvén waves. The evolution in this case was found to be much slower compared to the case of the DNLS soliton.

2.3 Chaos in Cometary Plasmas

So far our discussion has been confined to plasmas with only two species e.g., hydrogen plasma. Very often, we encounter multispecies plasmas with electrons, protons and heavy ions; the heavy ions, in laboratory plasmas, may be as impurities and in some natural plasmas as a genuine constituent, e.g., solar wind is composed of electrons, protons and α-particles (helium) and cometary plasmas have water group ions. To study the chaotic processes in such multispecies plasmas, starting from the corresponding multi fluid equations we had derived the evolution equation (Buti, 1992; Verheest and Buti,

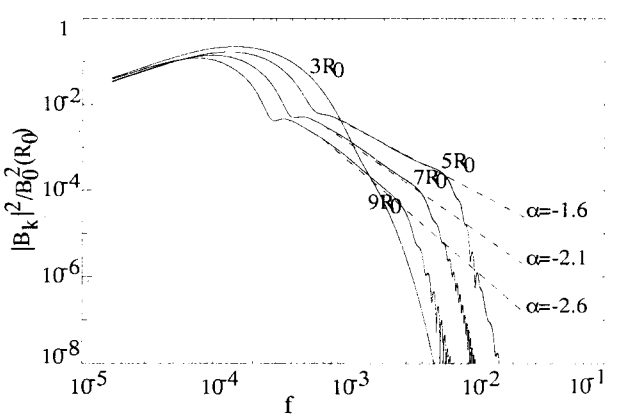

Fig. 2. Shows the power spectra for magnetic field at heliospheric distances 0.3 AU, 0.5 AU, 0.7 AU and 0.9 AU. The parameters used are same as for Fig.1. (from Buti et al., 1999a)

1992), which is given by:

$$\frac{\partial B}{\partial t} + \alpha \frac{\partial}{\partial x}\left(B \mid B \mid^2\right) \pm i\mu \frac{\partial^2 B}{\partial x^2} = 0. \tag{23}$$

with α and μ defined by:

$$\alpha = \frac{1}{4} \sum_s \frac{\rho_{so}^2 \left(1 - Z_s\, \delta\right)}{\left(\rho_{so} - \gamma_s P_s\right)}, \tag{24a}$$

$$\mu = \frac{1}{2} \sum_s \frac{\rho_{so}}{Z_s}, \tag{24b}$$

$$\delta = \sum_s \frac{\rho_{so} Z_s \gamma_s P_s}{\left(\rho_{so} - \gamma_s P_s\right)} \left[\sum_s \frac{Z_s^2 \rho_{so}^2}{\left(\rho_{so} - \gamma_s P_s\right)}\right]^{-1}, \tag{24c}$$

where subscript s refers to different species, γ is the ratio of the specific heat and Z is the charge to mass ratio. As a result of this, the localized stationary Alfvén waves that are driven by a harmonic driver can be represented by the following set of equations (Buti, 1992):

$$\frac{dB_y}{d\psi} = \frac{\partial H}{\partial B_z} + \frac{A}{2\,\mu} \cos\theta, \tag{25a}$$

$$\frac{dB_z}{d\psi} = -\frac{\partial H}{\partial B_y} + \frac{A}{2\,\mu} \sin\theta, \tag{25b}$$

$$\frac{\partial \theta}{\partial \psi} = \Omega, \tag{25c}$$

where A is the amplitude of the driver and H is the Hamiltonian given by,

$$H\left(\vec{B}\right) = \frac{1}{2}\alpha\left(1 - \beta\right)\left(B^2 - 1\right)^2 - \frac{\Lambda}{2}\left(\vec{B} - \hat{e}_y\right)^2, \tag{26}$$

with $\psi = (x - Vt)/\mu$ and

$$\Lambda = \frac{2(1-\beta)}{\mu}\left(\frac{V}{b_0^2} - \alpha\right) \tag{27}$$

To see the effect of the heavier species, here we will present the results of cometary plasma with oxygen ions as the third species. Hada et al. (1990) had earlier investigated the problem of Alfvénic chaos in driven Hamiltonian systems with only two species. Recently Chian et al. (1998) have looked into the problem of Alfvénic intermittent turbulence by using similar Hamiltonian approach but they also considered only 2-species plasmas.

For cometary plasma with 10% oxygen in abundance, Poincare maps, for the two-species and the three-species plasmas, are shown in Figs.3 and 4 respectively (Buti, 1992; 1996; 1997a). For both the figures, the driver is the left hand driver. Since all the parameters for both the figures are the same, Fig.4 shows the effect of the oxygen ions. Fig.3 shows that even for a weak driver corresponding to $A = 0.3$, or even for smaller A (not shown here), Alfvén waves in a 2 - species plasma (without any heavy ions) become chaotic.

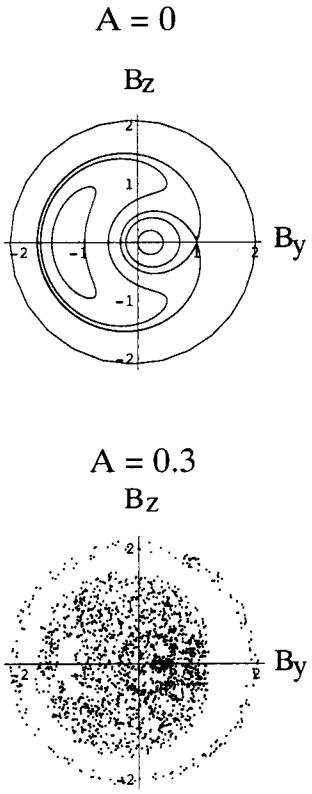

Fig. 3. Poincaré maps for a driven Alfvénic system in a 2-species plasma.

However, as shown in Fig.4, in the presence of the heavier oxygen ions, the chaos appears only when the driver is relatively much stronger. From comparison of these two figures, it is evident that the chaos is reduced due to the presence of the oxygen - in other words, the threshold for chaos goes up because of heavy ions. Physically this could be interpreted as the inertial stabilization due to the heavy ions.

2.4 Controlling Chaos in Dusty Plasmas

Dusty plasmas are prevalent in many cosmic as well as space plasmas such as planetary rings, planetary magnetospheres, cometary environment, interstellar medium etc. (Spitzer, 1978; Goertz, 1989; Northrop, 1992; Mendis and Rosenberg, 1994). Here we would like to distinguish between plasmas with a few dust grains and the plasmas where dust grains, satisfying the condition $N_d\ \lambda_d^3 >> 1$ (N_d being the density of charged dust grains and λ_d the Debye length), form the third constituent of the plasma. Only the latter ones we would define as dusty plasmas. Unlike the ordinary plasmas, dusty plasmas have very massive heavily charged dust grains. Moreover the charge fluctuations in dusty plasmas can be very significant. Nonlinear Alfvén waves in dusty plasmas are governed by (Verheest and Meuris, 1996),

$$\frac{\partial \vec{B}_\perp}{\partial t} + \alpha_1 \frac{\partial}{\partial x}\left(\vec{B}_\perp \mid \vec{B}_\perp \mid^2\right) + \mu_1 \left(\hat{e}_x \times \frac{\partial^2 \vec{B}_\perp}{\partial x^2}\right) \tag{28}$$

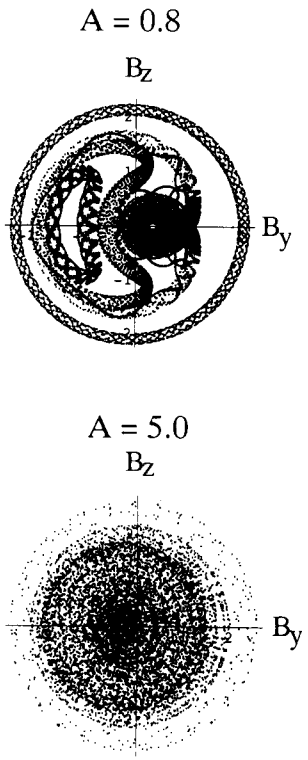

Fig. 4. Poincaré maps for a driven Alfvénic system in 3-species cometary plasma with water group ions.

$$+\delta_1 \vec{B}_\perp = 0.$$

Eq. (28) is same as the one for multispecies plasmas (Buti, 1992; Verheest and buti, 1992) except for the additional (last term) source term which is due to charge fluctuations of the dust grains. The co-efficients α_1, μ_1 and δ_1 for cold plasmas are given by:

$$\alpha_1 = \frac{1}{4\,g}, \tag{29a}$$

$$g = \sum_s \rho_s \,(V - U_s)\,, \tag{29b}$$

$$\mu_1 = \frac{1}{2g} \sum_s \frac{\rho_s \,(V - U_s)^3}{\Omega_s}, \tag{29c}$$

$$\delta_1 = \frac{1}{2g} \sum_s \sum_r \left(\rho_s\, \gamma_{sr} - \rho_r\, \gamma_{rs}\right) U_r, \tag{29d}$$

where ρ_s is the mass density , Ω_s is the cyclotron frequency and U is the drift velocity in equilibrium. Note that in the absence of any equilibrium drift i.e., for $U_s = 0$, the source term vanishes; in this case V reduces to the Alfvén speed ($V_A = (B_o/(4\pi\rho)^{1/2})$. For 3- species plasma with electrons, protons and heavy dust grains, these coefficients are simply given by,

$$\alpha_1 = \frac{1}{4}\left(1 + \frac{\rho_d}{(\rho_e + \rho_p)}\right)^{-1/2}, \tag{30a}$$

$$\mu_1 = \frac{1}{2g}\left(1 + \frac{\rho_d}{(\rho_e + \rho_p)}\right)^{-2}\left(1 + \frac{\rho_d\,\Omega_p}{\rho_p\,\Omega_d} + \frac{\rho_e\,\Omega_p}{\rho_p\,\Omega_e}\right), \tag{30b}$$

$$\delta_1 = 0. \tag{30c}$$

In Eqs.(30), the subscripts e, p and d represent electrons, protons and dust grains respectively. For 2-species plasma i.e., for $N_d = 0$, note that $V = g = 1$, $\alpha_1 = 1/4$ and $\mu_1 = 1/2$. In writing Eqs.(29), we have made use of the charge neutrality condition, i.e., $(N_e + Z_d N_d) = N_p$. In the presence of an external driver, Eq. (28) gets modified; the source term $S(\vec{B}_\perp, x, t)$ appears on the right hand side of Eq. (28) (Hada et al., 1990). For a plane circularly polarized driver i.e., for S = A exp (i k ψ), Eq. (28) can be written in terms of the Hamiltonian of the system (Buti, 1992; 1997), namely

$$\frac{dB_y}{d\psi} = -\frac{\partial H}{\partial B_z} - \frac{A}{2\,\mu_1}\cos\theta, \tag{31a}$$

$$\frac{dB_z}{d\psi} = \frac{\partial H}{\partial B_y} - \frac{A}{2\,\mu_1}\sin\theta, \tag{31b}$$

$$\frac{\partial\theta}{\partial\psi} = \Omega, \tag{31c}$$

where $\psi = (x - V\,t)\,/\,2$, A and Ω as the amplitude and the frequency of the driver and H the Hamiltonian that is given by,

$$H\left(\vec{B}\right) = \frac{1}{2}\frac{\alpha_1}{\mu_1}\left(B^2 - 1\right)^2 - \frac{\Lambda_1}{2}\left(\vec{B} - \hat{e}_y\right)^2, \tag{32}$$

with

$$\Lambda_1 = \frac{2}{\mu_1}\left(\frac{V}{b_0^2} - \alpha_1\right) \tag{33}$$

and b_0 as the asymptotic value of B.

As mentioned earlier, dusty plasmas are observed in nebulas, planetary rings, planetary magnetospheres and cometary environment. We have solved Eq. (31) numerically for the case of rings of Saturn and for the cometary cases. In these systems (i.e., the Saturn rings and comets), dust grain size is typically a few microns and dust mass is of the order of 10^{12} m_p. The dust grains carry very high charges (Mendis and Rosenberg, 1994); typically $Z_d \sim (10^3 - 10^4)e$. However the dust number densities could be as low as $(10^{-8} - 10^{-6})\,N_p$. For these parameters α_1 and μ_1 simply reduce to,

$$\alpha_1 \simeq \frac{1}{4}\left(\frac{\rho_p}{\rho_d}\right)^{1/2} \tag{34}$$

and

$$\mu_1 \simeq \frac{1}{2}\frac{\rho_p\,\Omega_p}{\rho_d\,\Omega_d} = \frac{1}{2}\frac{N_p}{N_d\,Z_d}. \tag{35}$$

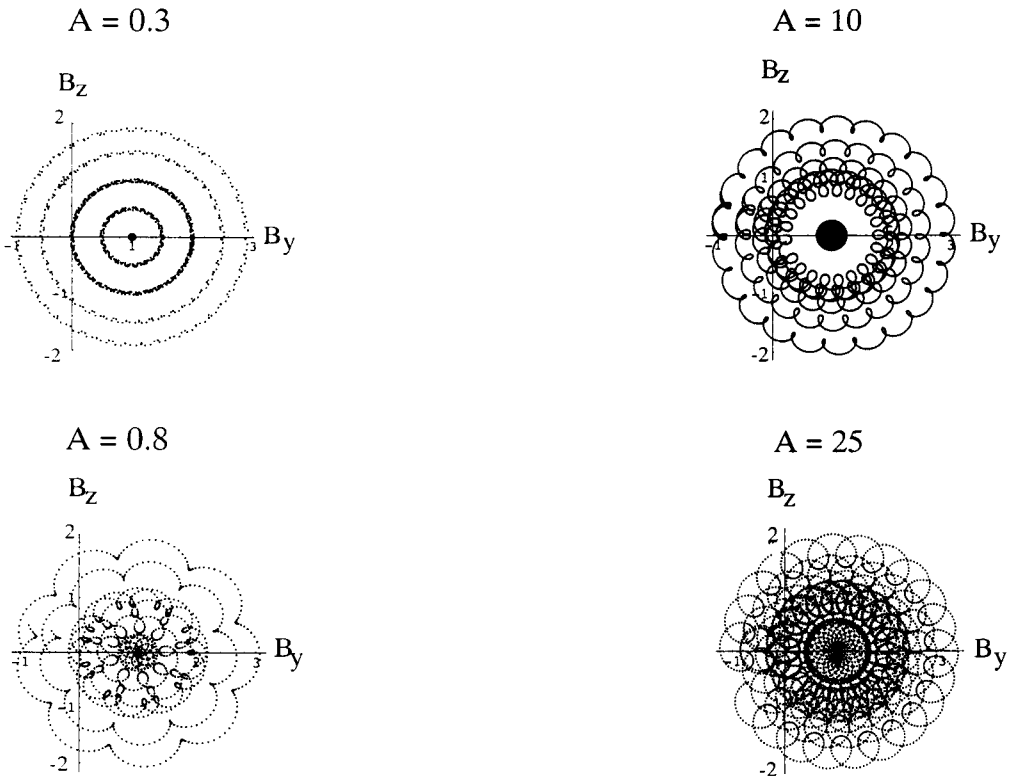

Fig. 5. Same as Fig.3 but with the dust grains with $N_d/N_p = 1.7 \times 10^{-4}$, $Z_d = 10^3$, $m_d / m_p = 10^{12}$. (from Buti, 1997)

Fig. 6. Same as Fig.5 but for Saturn Rings with $N_d/N_p = 4 \times 10^{-8}$, $Z_d = 10^4$. (from Buti, 1997)

Thus it is apparent that the crucial parameters, governing the nonlinear dynamics, are the mass density and the charge of the dust grains. Strictly speaking one should consider the size distribution of the dust grains but this has not been incorporated in the derivation of Eq.(28).

The results of numerical computations are shown in Figs.5 and 6. Fig.3 shows that even for a weak driver corresponding to $A = 0.3$, Alfvén waves in a 2 - species plasma (without the dust grains) become chaotic. However in dusty plasmas as shown in Fig.5 for cometary plasmas and in Fig.6 for Saturn rings, Poincare maps do not show any chaos. One gets only periodic orbits even for strong drivers with amplitudes which are order of magnitude larger compared to the one for 2 - species plasma. From these results (Figs.5 and 6), we can straightaway conclude that the chaos in Alfvénic systems simply disappears due to the presence of massive dust grains. The procedure for controlling chaos in nondissipative systems, discussed here, is very different than the one presented by Ott et al. (1990) for the dissipative systems.

2.5 Spatio-Temporal Evolution of Driven Alfvén waves

In sections 2.2 and 2.3, we have discussed the conditions under which *Localized Stationary* Alfvén waves, driven by an external driver, can become chaotic. In this section, we will deal with the spatio-temporal evolution of these driven Alfvén waves. For stationary waves, we could reduce the governing driven DNLS equation to a set of ordinary differential equations (cf. Eqs.(31)) but for the nonstationary waves, we have to work with the nonlinear partial differential equation instead, namely the driven DNLS equation:

$$\frac{\partial B}{\partial t} + \frac{1}{4\,(1-\beta)} \frac{\partial}{\partial x} \left(B \mid B \mid^2 \right) \pm \frac{i}{2} \frac{\partial^2 B}{\partial x^2} = a\, e^{i(\kappa x - \Omega t)}, \quad (36)$$

where a is the amplitude of the driver. This driven DNLS equation, like the MDNLS Eq.(16), is not an integrable equation. As shown above, the external driver in Eq.(36) simply acts as a source, which kills the coherent properties of the solitons (Nocera and Buti, 1995; 1996; 1997; 1998). Ghosh and Papadopoulos (1987) had thoroughly investigated the spatio-temporal evolution in the presence of an exponential driver due to the linear growth provided by the ion beam resonance with one unstable k-mode. On the other hand, harmonic driver has been used by a number of investigators (Hada et al., 1990; Buti, 1992, 1997; Chian et al., 1998), who used a low-dimensional Hamiltonian approach to study the localized temporal evolution. We plan to extend the results obtained by these authors by incorporating a large number of degrees of freedom (2048) to look into the spatio-temporal evolution of Alfvénic systems in general and in particular theit evolution to turbulence. In connection with the solar wind, it certainly would be more realistic to take a 'pulse' type driver to represent the effects of the solar flare

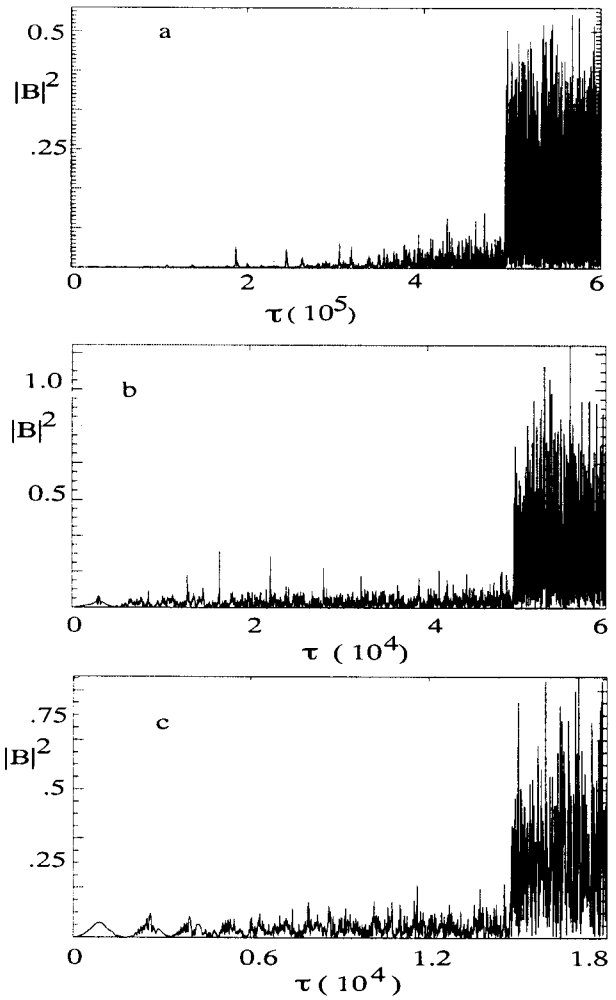

Fig. 7. Transition of left-hand polarized soliton to chaos a) at $\tau \sim 5 \times 10^5$ for $A = 0.003$, b) at $\tau \sim 5 \times 10^4$ for $A = 0.03$, c) at $\tau \sim 1.48 \times 10^4$. for $A = 0.1$. Note that $\tau = t/144$.

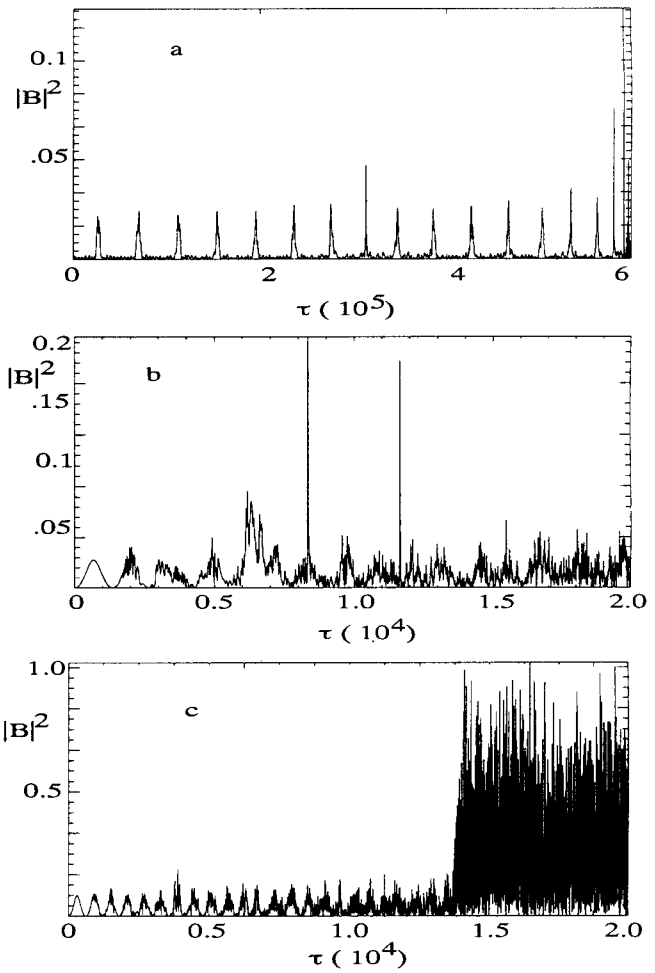

Fig. 8. Time series for evolution of RHP soliton at $x = L/8$ for a) $A = 0.01$, b) $A = 0.1$, c) $A = 0.5$.

and/or solar radio burst. We are looking into the dynamical behaviour of the Alfvén waves in the presence of a pulse type driver; these results will be reported in a future publication. Unlike the DNLS Eq.(7), Eq.(36) can not be solved analytically. This equation is solved by spectral-collocation method with periodic boundary conditions. For the initial condition we take a solitary Alfvén wave packet, namely

$$B\ (x,\ t = 0)\ =\ \frac{(2^{1/2} - 1)^{1/2}\ B_s\ e^{i\theta\ (x)}}{[2^{1/2}\ \cosh\ (2\ V_s\ x)\ -\ 1]^{1/2}}, \qquad (37)$$

where B_s is the amplitude of the soliton,

$$\theta\ (x, t = 0) = -V_s x + 3\tan^{-1}[(2^{1/2} + 1)\tanh(2V_s x)] \qquad (38)$$

and V_s is the soliton speed defined by,

$$V_s\ =\ \frac{(2^{1/2} - 1)\ B_s^2}{8\ |\ (1\ -\ \beta)\ |}. \qquad (39)$$

Note that Eq. (37) is the super-Alfvénic soliton solution of Eq.(7) in the wave frame of reference (Verheest and Buti, 1992). The reason for picking up the DNLS soliton solution as the initial condition is the following: Locally in the regions closer to the sun, where Alfvén waves are believed to be generated, DNLS is a good representation of the Alfvén waves. Moreover one of the basic properties of any evolution equation, e.g., DNLS equation, which can be solved exactly by means of the Inverse Scattering Transform method (Kaup and Newell, 1978), is to transform any localized initial condition to a soliton solution. Dawson and Fontan (1988) had numerically solved the DNLS equation with an initial modulated Gaussian packet and confirmed its decay into soliton solution.

For $\beta < 1$, from our simulations, We observe that the LHP soliton very quickly, even for a relatively weak driver, loses its coherent properties and goes into a chaotic state (Buti and Nocera, 1999a). For numerical calculations, we have scaled Eq.(36) and have taken $L = 800$ (L is the simulation box length), $\beta = 0.1$, $\kappa = 2\pi/100$, $\Omega = 10^{-4}$ and $B_s = 0.5$. The values of κ and Ω used here are arbitrary. We could pick up different numbers but the resultant qualitative behaviour does not change. This driver could be easily taken

as another coexisting wave; for this κ and Ω however would be related through its dispersion relation. For the parameters used for the present calculations, the speed of the initial soliton, in the solar wind frame of reference, turns out to be $1.025V_A$. The super-Alfvénic nature of the soliton is simply because we have used the super-Alfvénic solution (37) for the DNLS Eq.(7). The corresponding width of the soliton, which is given by $1/(2V_S)$, is $\sim$ 20 ion inertial lengths. We believe that such large amplitude pulses, distributed over very many ion inertial lengths, have been observed in space plasmas.

Fig.7 shows the time evolution of the driven left-hand soliton for various amplitudes of the harmonic driver. We find that even for an extremely weak driver with amplitude $A = 0.003$, LHP wave becomes chaotic at $\tau \sim 5 \times 10^5$ (cf. Fig 7a). Note that $\tau = t/(144)$ and A is the scaled amplitude ; $A = (12^{5/2})a$. The time-series corresponding to somewhat stronger drivers namely, A = 0.03 and 0.1 are shown in Figs.7b and 7c. From these two figures, we see that the chaos sets in at $\tau \sim 5 \times 10^4$ and at $\tau \sim 1.48 \times 10^4$ for $A = 0.03$ and $A = 0.1$ respectively. It is interesting to note that the time at which Alfvénic system becomes chaotic scales as A^{-1}.

In contrast, the RHP soliton is found to be much more robust as expected from the DNLS equation. From the stability analysis of the DNLS equation, we know that the modulational instability crucially depends on the sign of the product of the co-efficients of nonlinear and dispersive terms of the DNLS equation. For systems with $\beta < 1$, the case we are considering, left-hand one is unstable and the right-hand one is stable. Time evolution, of RHP soliton at $x = L/8$ (L being the length of the simulation box),is shown in Fig.8 for $A = 0.01$ (Fig.8a), 0.1 (Fig.8b) and 0.5 (Fig.8c). Unlike the case of LHP soliton, RHP goes into a chaotic state only when it is driven by a real strong driver with $A = 0.5$. In case of weaker drivers (cf. Fig.8a, 8b), only low level turbulence is generated which is seen in between the perturbed solitons. This is further confirmed by Fig.9, which shows the spatio-temporal evolution of the right-hand soliton governed by the driven DNLS for the parameters identical to the case of the left-hand soliton. For the weak turbulence, shown in Fig.8a, we have calculated the space as well as time correlations and we find that the time correlations are destroyed much more quickly compared to the space correlations (Buti and Nocera, 1999b).

2.6 Turbulence through Chaotic Channels

For the chaotic states shown in Figs. 7a-7c and in Fig.8c, we have calculated the power spectra for the magnetic field fluctuations. The results are shown in Fig.10. For LHP, with a very weak driving source ($A = 0.003$), we find an exponentially decaying energy spectrum. On the other hand, for the chaotic states shown in Fig.7c and Fig.8c, the mag-

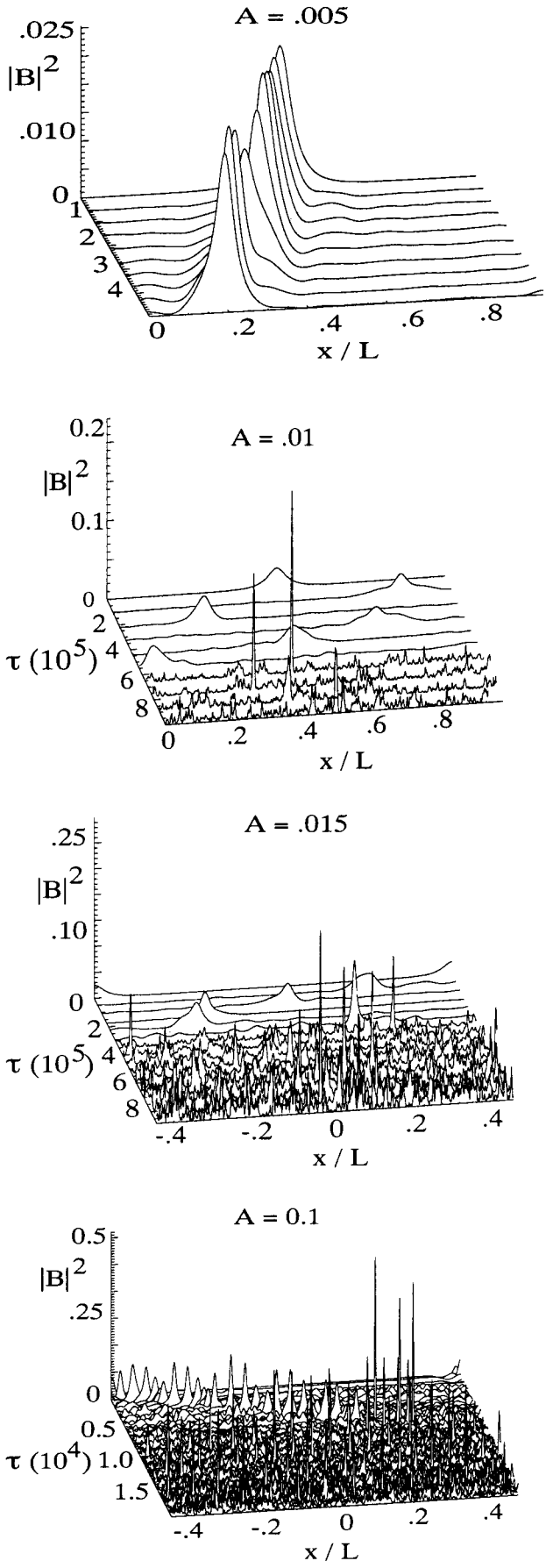

Fig. 9. Spatio - temporal evolution of RHP soliton for a) $A = 0.005$, b) $A = 0.01$, c) $A = 0.015$, d) $A = 0.1$

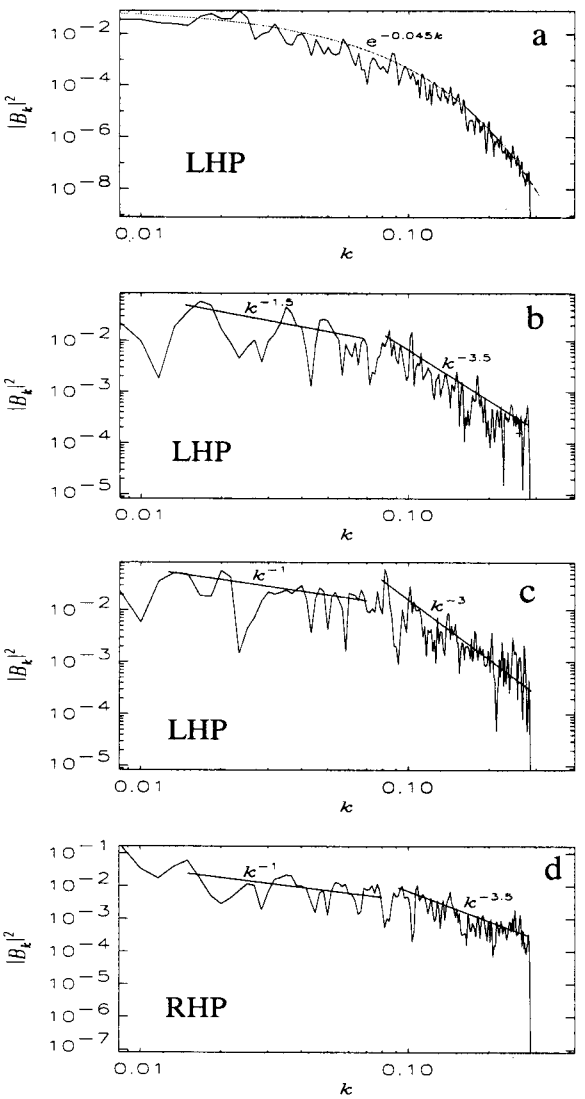

Fig. 10. Shows Spectra for magnetic field turbulence generated through chaos for a) LHP with $A = 0.003$, b) LHP with $A = 0.03$, c) LHP with $A = 0.1$ and d) RHP with $A = 0.5$.

netic energy scales as k^{-1} and for the case of chaos shown in Fig.7b, it scales as $k^{-1.5}$. The latter corresponds to the Kraichnan (1965) spectrum of hydromagnetic turbulence. In all the three cases we do see a break in the spectral index. These results have a lot of resemblance with the observations of solar-wind turbulence reported by Bavassano et al. (1982). These results are in contrast to the general feeling that the turbulence can be generated only by an infinite (or a very large) number of modes. However one can view the scenario presented here as analogous to the system with a finite but large number of modes. This is indicated by Figs.10a-10c, which show that the energy is distributed into a few tens of modes. It is worth noting that the turbulent spectra, presented in Fig.10, appear through chaotic channels only.

2.7 Collapse and Self-Organization in Alfvénic Systems

Let us revisit the evolution of an RHP soliton driven by a harmonic driver with amplitude $A = 0.01$. Its evolution at $\tau \sim 6 \times 10^5$ is shown in Fig.11a where we see a highly peaked soliton with $|B_{max}|^2 \sim 0.2$ coexisting with a very weak background turbulence. The width of this soliton, which is given by $(2\ V_S)^{-1}$, turns out to be approximately $1.7 R_L$ (R_L being the Larmor-radius). Thus we are observing the 'collapsed' soliton. For the parameters used in section 2.5, R_L in our dimensionless units (V_A/Ω_i) is 0.4. Similar collapsed soliton for the case of the driver with $A = 0.1$ appears much earlier at $\tau \sim 1.4 \times 10^4$ and with much larger amplitude $|B_{max}|^2 \sim 0.5$ (shown in Fig.11b). The DNLS soliton, in our case is collapsing mainly due to its interaction with the driver. This is an altogether different process compared to the collapse of an NLS soliton which occurs because of multi-dimensional aspects (Zakharov, 1984) . We must bear in mind that while dealing with systems involving such small scale lengths, kinetic effects should be properly included. We are looking into these aspects by means of hybrid simulations. These results will be reported in a separate publication (Buti et al., 1999b).

To ascertain the cause of the collapse of the DNLS soliton, we introduced a jump $\Delta\Phi = 2.876$ in the phase $\Phi = (\kappa x - \Omega t)$ of the driver at $\tau = 5.3 \times 10^5$ and then integrated Eq.(36) to determine its evolution between $\tau = 5.3 \times 10^5$ and $\tau = 8 \times 10^5$. The resulting evolution at $\tau = 8 \times 10^5$ is shown in Fig.12. Once again we see the bifurcation of the solution from one peak of Fig.11 to four peaks of Fig.12. Here we find a much bigger surprise. The four narrow pulses in Fig.12 turn out to be the four solitons of our original non-driven DNLS equation (7). This is a clear demonstration of Self-Organization phenomena. The energy stored in the original one soliton, because of its interaction with the driver, is redistributed into the final four solitons which have speeds four times that of the original soliton i.e., $4\ V_s$.

In order to determine whether the self-organization / pattern formation are characteristics of the initial soliton condition or of the evolution equation itself i.e., the DNLS, we had repeated our calculations for an initially structureless DNLS equation. Once again we found that the right-hand solutions are stable and appear as elliptic oscillations (Buti, 1998; Nocera and Buti, 1998). The left-hand solutions, on the other hand, do start with elliptic solutions but unlike RHP solutions they are found to be unstable. These ellipitic solutions in turn bifurcate into the bell-shaped wave packets. The latter (bell-shaped) solution is also not stable. The elliptic and the bell-shaped solutions appear alternatively (see Fig.13). So, we conclude that the self-organization is generic to the DNLS equation, and is independent of the initial conditions.

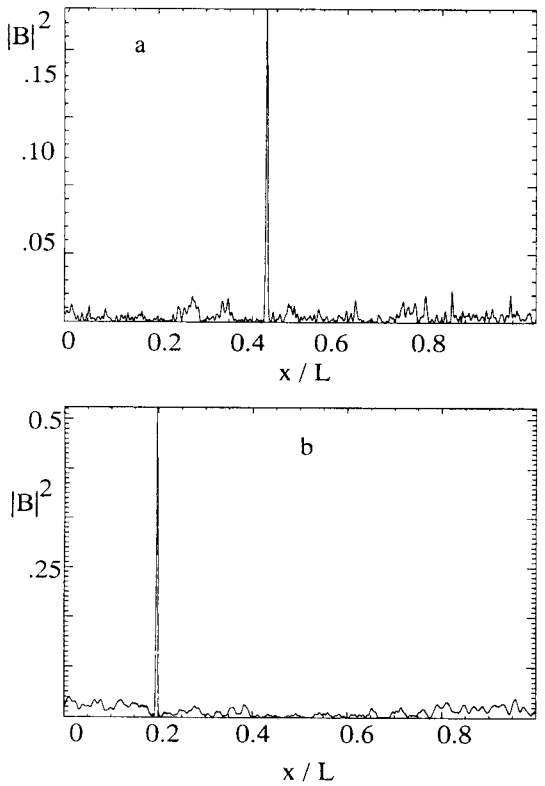

Fig. 11. Collapse of RHP soliton due to the driver with a) $A = 0.01$ at $\tau \sim 6 \times 10^5$ and b) $A = 0.1$ at $\tau \sim 1.4 \times 10^4$.

2.8 MHD Simulations

As mentioned above, for large amplitude waves ($\delta B/B \geq 1$), the approximations made in the derivation of the DNLS / MDNLS equations become invalid because the derivation includes terms only up to cubic nonlinearities. Moreover these evolution equations are not valid for $\beta \sim 1$. For $\beta \sim 1$, coupling between Alfvén waves and ion acoustic waves becomes significant. One could overcome these limitations by doing simulations. For this purpose let us go back to the full set of Hall-MHD equations, namely Eqs. (2) - (6). These equations are solved by using periodic boundary conditions and by taking the DNLS soliton solution, given by Eqs. (37) - (39), as an initial condition (Buti et al., 1998; Velli et al., 1999). Unlike fusion plasmas, some of the space plasmas have $\beta > 1$. In the solar wind, β, T_e and T_i (T_e, T_i being the electron and the ion temperature) all vary with the heliospheric distance. In particular, β spans the entire range from $\beta < 1$ to $\beta > 1$. To investigate the stability of the initial DNLS soliton, we have done the simulations for different values of β; spatio - temporal evolutions of the RHP solitons are shown in Figs. 14 and 15. We observe a wave train on the leading edge for $\beta < 1$ (cf. Fig.14a) and on the trailing edge for $\beta > 1$ (cf. Fig.14b). However in both cases the amplitude of the soliton goes down. It is interesting to compare this with the evolution of the magnetic field of the LHP initial soliton. In the latter case wave train appears on the leading edges (Buti et al., 1998) for $\beta < 1$ as well as for

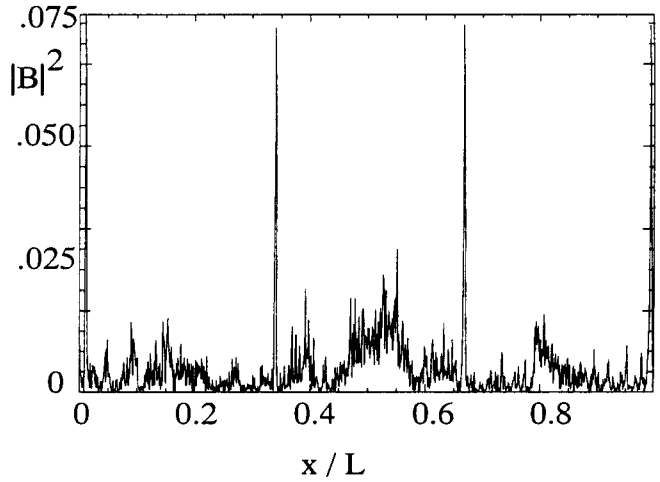

Fig. 12. Shows redistribution of energy into four solitons at $\tau \sim 8 \times 10^5$ due to a phase shift of 2.678 imparted to the driver at $\tau \sim 5.3 \times 10^5$.

$\beta > 1$. Moreover, in this case the amplitude was found to increase (decrease) for $\beta < 1 (> 1)$ as the soliton evolved. We had observed similar behaviour (Velli at al., 1999) for plasmas with much smaller β e.g., solar corona with $\beta = 0.05$. Buti et al. (1998) had considered the case with much higher β also and showed that for $\beta = 3$ for the RHP soliton, by $t = 5000$ ion cyclotron periods, the wave train disappears. So it is pretty obvious that the soliton is disrupted simply because of the higher order nonlinearities that are neglected in the DNLS / MDNLS equations. In fact we had shown (Velli et al., 1999) that the disruption time scales as B_s^{-4}.

The density fluctuations that are taken as sort of static in the DNLS description, are also found to evolve (see Fig.15). Unlike the driven soliton that evolves into fully developed turbulence (see Fig.10) through chaotic channels, in all the cases that we have considered so far (Buti et al., 1998; Velli et al., 1999) for our MHD simulations, we find that neither the higher order nonlinearities nor the coupling of magnetic field and density fluctuations lead to Alfvénic turbulence. We are persuing the MHD as well as hybrid simulations with larger-amplitude solitons to see if there is any possibility of generating turbulence through nonchaotic channels. Velli et al. (1999) had looked into the soliton evolution in the expanding solar wind by using the Expanding Box Model. They found that the nonlinear effects dominate over the expansion. Moreover their simulations showed evolution with expansion to be very similar to the one obtained by Buti et al. (1999a) by solving the inhomogeneous DNLS (MDNLS) equation.

3 CHAOTIC LOWER-HYBRID WAVES

As mentioned earlier, besides Alfvén waves, lower - hybrid waves are also observed in a variety of plasmas. It is known that these waves can become unstable due to free energy source provided by (Lakhina and Buti, 1996): a) a gas of

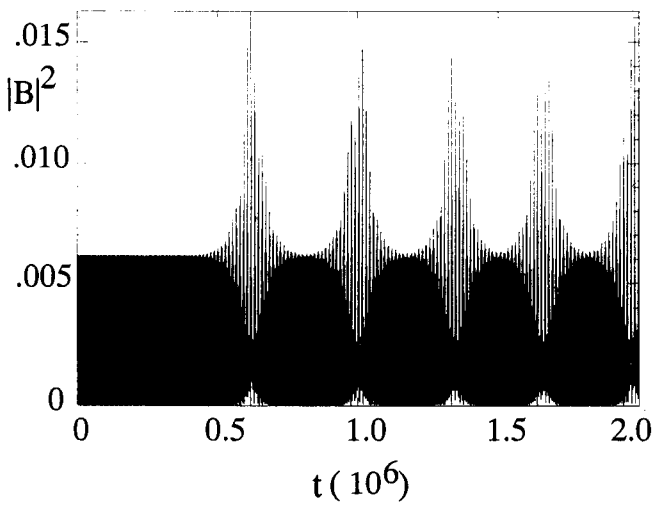

Fig. 13. Self-organization and pattern formation for an LHP wave with vanishing initial condition.

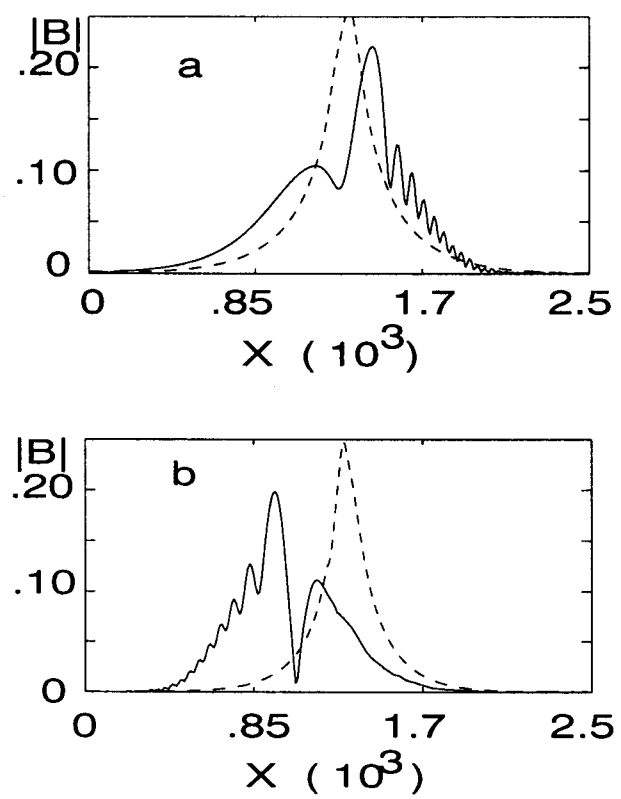

Fig. 14. Evolution of magnetic field fluctuations for a RHP soliton for a) $\beta = 0.3$, and b) $\beta = 1.5$ at $t = 0$ (dashed line) and $t = 5000$ (solid line).

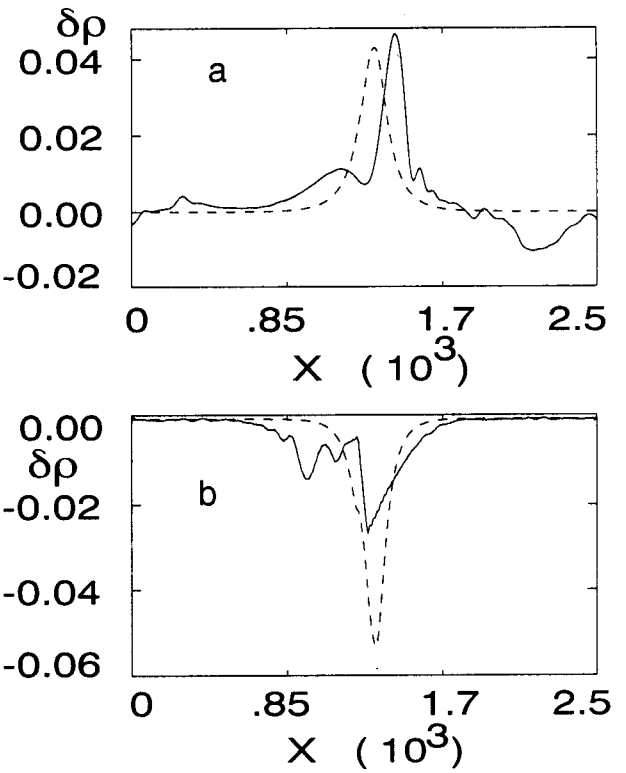

Fig. 15. Evolution of density fluctuations for a RHP soliton for a) $\beta = 0.3$, and b) $\beta = 1.5$ at $t = 0$ (dashed line) and $t = 5000$ (solid line).

hot nonthermal electrons, streaming relative to cooler population of electrons, along the external magnetic field; b) relative drift between electrons and ions perpendicular to the magnetic field; c) ions with ring type distributions in non-drifting plasmas. Clearly, the growth of the instability would depend on the nature of the free energy source as well as the plasma constituents but if the fields generated by these instabilities can exceed certain threshold, which also depends on the nature of the plasma under consideration, the system can become chaotic. For simple two - species plasmas, estimates of this threshold field for the lower - hybrid waves were given by Karney and Bers (1977) and Karney (1978). The threshold electric field, obtained by Karney (1978) for the lower - hybrid waves, is given by:

$$E_t = B_0\, \Omega_i^{1/3}\, \omega_{LH}^{2/3}/(4ck), \tag{40}$$

where B_0 is the external uniform magnetic field, Ω_i is the ion cyclotron frequency and ω_{LH} is the lower - hybrid frequency that is given by,

$$\omega_{LH} = \omega_{pp}\,(1 + \frac{m_p\, k_{||}^2}{m_e\, k^2})^{1/2}\,(1 + \frac{\omega_{pe}^2}{\Omega_e^2})^{-1/2}. \tag{41}$$

For $k_{||}/\ k \leq (m_e/m_p)^{1/2}$, $\omega_{pe}^2 \gg \Omega_e^2$, $\omega_{LH} \sim (\Omega_e\ \Omega_p)^{1/2}$. We had investigated the propagation of chaotic lower - hybrid waves in multi - species plasmas to explore

the possibility of anomalous particle acceleration in the following two entirely different systems.

3.1 Chaotic Acceleration of Cometary Ions

In the region of interaction between the solar wind and the comet, we have to deal with the multi - species plasmas, at least three if we take into account only the most dominant cometary ions. The latter after their ionization are picked up by the solar wind; in the pick - up region, these ions are supposed to have ring type distribution, namely

$$f_{0i} = \frac{N_i}{2\pi^{3/2}\, V_{ti}\, U_{\perp 0}}\, \delta\,(V_\perp - U_{\perp 0})\, \exp[-\frac{(V_{||} - U_i)^2}{V_{ti}^2}], \quad (42)$$

where N_i and V_i are the density and thermal velocity of the ions and $U_i = U_{||0}$ is the parallel drift velocity of the ions in the solar wind frame. We notice that the distribution function given by Eq. (42) provides two sources of free energy, namely the relative drift between the cometary ions and the solar wind protons and secondly the ring in velocity space. Both these sources lead to lower - hybrid instability whose growth rate is given by (Buti and Lakhina, 1987) :

$$\gamma = \alpha\, \omega_{LH}\, [(N_i\, m_p)\, /\, (N_p\, m_i)/(1 + \frac{m_p\, k_{||}^2}{m_e\, k^2})]^{2/5}, \quad (43)$$

where α is a constant of order unity and ω_{LH} is the lower - hybrid frequency given by Eq. (41). The subscripts e, p and i refer to electrons, protons and the heavier ions. The saturated electric field associated with this instability turns out to be,

$$E_s = [2\pi\, m_i\, N_i\, U_{\perp 0}^2/(1 + \omega_{pe}^2/\Omega_e^2)]^{1/2}. \quad (44)$$

It is interesting to note that this instability arises only because of the cometary ions since $\gamma \to 0$ for $N_i = 0$. This system could become chaotic if $E_s > E_t$; E_t is the threshold electric field that is given by Eq.(40).

Furthermore these chaotic fields would lead to anomolous acceleration of cometary ions provided the time (t_a) required to accelerate the ions to the maximum energy attainable from these fields is much smaller than the time (t_d) in which they drift out of the chaotic region. As shown by Buti and Lakhina (1987), both these conditions can be satisfied in the ion pick - up regions of comets Halley as well as Ziacobini - Zinner. They also showed that in case of comet Halley, the O^+ ions (the most dominant ions) can be accelerated to maximum energies of the order of 32 Mev whereas the observed energies for heavy ions were found to be in the range 45 - 270 Kev. A part of this energy provided by the chaotic electric field is used up for heating the plasma and the rest for accelerating the particles. Similarly in the case of comet Giacobini - Zinner, water group ions with energies exceeding 300 Kev were observed and the model of Buti and Lakhina (1987) leads to maximum energies, given to these ions by the chaotic fields associated with the lower - hybrid waves, of the order of 2 Mev. From these figures, one may draw the conclusion that the chaos generated by the observed lower - hybrid waves is responsible for the observed energetic heavy ions in the vicinity of comets Halley and Giacobini - Zinner.

3.2 Chaotic Acceleration in the Solar Corona

The hot (nonthermal) electron beams, escaping the injection region (top of the coronal loop) along the coronal magnetic field lines, impinge on the cooler chromospheric plasma at the foot of the coronal loop and excite the lower hybrid waves (Lakhina and Buti, 1996). Unlike the lower - hybrid waves discussed in Sec. 3.1, here the source of free energy is the relative drift between the hot electrons and the cold electrons / ions parallel to the magnetic field. This drift can drive the lower - hybrid waves unstable if $U_h > U_{ph}$ (Lakhina and Buti, 1996) ; U_h and U_{ph} being the parallel beam (hot electron) velocity and the phase velocity of the wave. This instability can generate saturated electric field that is given by:

$$E_{sat} = (2\pi m_e N_h/\Delta)^{1/2}(U_h - U_{ph}). \quad (45)$$

where

$$\Delta = 1 + f_c\, \omega_{pc}^2/\Omega_e^2 + \omega_{ph}^2/(k^2 V_{th}^2). \quad (46)$$

Here the subscripts c and h refer to the cold and the hot electrons and ω_{ps} (s = c or h), Ω_e are the electron plasma and cyclotron frequencies. Once again, for the production of chaotic lower hybrid waves, we must satisfy the condition $E_{sat} > E_t$. The threshold electric field E_t is given by Eq.(40). For the solar coronal plasma parameters, namely $N_c = 8 \times 10^{11} cm^{-3}$, $T_c = 3.5 \times 10^4 K$, $B_0 = 100G$, $T_h/T_c = 100$, $U_h/V_{th} = 4$ and $N_h/N_c \sim 0.005$, it was shown by Lakhina and Buti (1996) that the condition for stochasticity can be satisfied for a wide range of wave lengths. Consequently, lower hybrid waves can lead to stochastic acceleration of ions in the coronal loops. The maximum energy gained by the protons from such stochastic acceleration process was found to be $\sim 0.25 - 1.125$ MeV and the energy picked up by the singly charged heavier ions would exceed these values by a factor of $(m_i/m_p)^{5/3}$.

4 Discussion and Conclusions

The coherent properties of the DNLS solitons are destroyed by a variety of sources, e.g., inhomogeneities in the plasma densities and the magnetic fields, coupling of the magnetic field and the density fluctuations, higher order nonlinearities that are neglected in the derivation of the evolution equation and by some external source like a harmonic driver. In confirmation with the criteria for the occurence of the modulational instability, for $\beta < 1$, the right-hand polarized solitons are found to be much more robust compared to the left-

hand polarized ones. However both, under different conditions can lead to chaotic Alfvén waves and the chaos in turn leads to Alfvénic turbulence. The turbulence, with k^{-1} spectra, is observed only in case of driven Alfvén waves. To our knowledge, the chaotic route to Alfvénic turbulence, with k^{-1} spectra, is reported for the first time. The power spectra of the magnetic field is found to be similar in nature to the one observed in the solar wind. The phenomena of self-organization and collapse are also observed during the dynamical evolution of the Alfvén waves.

To incorporate the nonlinear damping and the other kinetic effects that become significant when $\beta \sim 1$, we have investigated the evolution of the DNLS soliton by hybrid simulations. We find that the soliton decays much faster for Alfvénic systems with $\beta \sim 1$ compared to the ones with $\beta << 1$. The other results from our hybrid simulations will be reported in a forthcoming paper (Buti et al., 1999b). The chaotic lower hybrid waves provide an efficient source for the preferential acceleration of the heavier ions in the cometary as well as the solar coronal plasma.

Acknowledgements. The research conducted at the Jet Propulsion Laboratory, California Institute of Technology, was performed under contract to the National Aeronautics and Space Administration. I would like to acknowledge the financial support from the National Research Council. I would also like to express my gratitude to all my co-authors of all the contributions used for the present review.

References

Ashour-Abdalla, M. and Baker, D.N., Chaos and Stochasticity in Space Plasmas, *Geophys. Res. Lett., 18*, 1573, 1991.

Bavassano, B., Dobrowolny, M., Mariani, F. and Ness, N.F., Radial evolution of Power Spectra of Interplanetary Alfvénic Turbulence, *J. Geophys. Res., 87*, 3617, 1982.

Belcher, J. W. and Davis, L., Large amplitude Alfvénic waves in the interplanetary medium, *J. Geophys. Res., 76*, 3534, 1971.

Burlaga, L.F., Multifractal Structure of Speed Fluctuations in Recurrent Streams at 1 AU and near 6 AU, *Geophys. Res. Lett., 18*, 1651, 1991a.

Burlaga, L.F., Intermittent Turbulence in the Solar Wind, *J. Geophys. Res., 96*, 5847, 1991b.

Buti, B., Stochastic and Coherent Processes in Space Plasmas, in *Cometary and Solar Plasma Physics,* Ed. B. Buti, World Scientific, Singapore, 1988.

Buti, B., Nonlinear and Chaotic Alfvén waves, in *Solar and Planetary Plasma Physics,* Ed. B. Buti, p 92 , World Scientific, Singapore, 1990.

Buti, B., Nonlinear Alfvén Waves in Inhomogeneous Plasmas, *Geophys. Res. Lett., 18*, 809, 1991.

Buti, B., Chaotic Alfvén Waves in Multispecies Plasmas *J. Geophys. Res., 97* , 4229, 1992.

Buti, B., Solitary Alfvén Waves in Inhomogeneous Streaming Plasmas, *J. plasma Phys., 47*, 39, 1992a.

Buti, B., Chaos and Turbulence in Solar Wind, *Astrophys. Space Sci., 243*, 33, 1996.

Buti, B., Control of Chaos in Dusty Plasmas, *Phys. Lett. A, 235*, 241, 1997.

Buti, B., Chaos and its Implications, *Pramana (Jou. of Physics), 49*, 93, 1997a.

Buti, B. Evolution and Control of Chaos in Plasmas, in *Nonlinear Dynamics and Computational Physics*, Ed. V.B. Sheorey, p 177, Narosa publisher, London , 1998.

Buti, B. and Lakhina, G.S., Stochastic Acceleration of Cometary Ions by Lower Hybrid Waves, *Geophys. Res. Lett., 14*, 107, 1987.

Buti, B., Jayanti, V., Viñas, A. F., Ghosh, S., Goldstein, M. L., Roberts, D. A., Lakhina, G. S., and Tsurutani, B. T., Nonlinear Evolution of Alfvénic Wave Packets, *Geophys. Res. Letts., 25*, 2377, 1998.

Buti, B., Galinski, V.L., Shevchenko, V.I., Lakhina, G.S., Tsurutani, B.T., Goldstein, B.E., Diamond, P. and Medvedev, M.V., Evolution of Nonlinear Alfvén Waves in Streaming Inhomogeneous Plasmas, *Astrophys. J., 523*, in press (Oct.!), 1999a.

Buti, B., Liewer, P.C., Goldstein, B.E. and Velli, M., to be submitted, 1999b.

Buti, B. and Nocera, L., Chaotic Alfvén Waves in the Solar Wind in *Solar Wind Nine, AIP Proceedings, 471*, Eds. S. Habbal et al., p. 173, American Institute of Physics, 1999a.

Buti, B. and Nocera, L., Evolution and Self-Organization of Alfvénic Wave Packets, *Phys. Plasmas, to appear*, 1999b.

Chian, A.C.-L., Borotto, F.A. and Gonzalez, W.D., Alfvén Intermittent Turbulence Driven by Temporal Chaos, *Astrophys. J., 505*, 993, 1998.

Contopoulos, G., The Transition to Chaos in Galactic Models of Two and Three Degrees of Freedom, in *Chaos in Astrophysics, ed. J.R. Buchler et al., Dordrecht: Reidel*, 259, 1985.

Dawson, S.P. and Fontán, C.F., Soliton Decay of Nonlinear Alfvén Waves: Numerical Studies, *Phys Fluids, 31*, 83, 1988.

Ghosh, S. and Papadopoulos, K., The Onset of Alfvénic Turbulence, *Phys. Fluids, 30*, 1371, 1987.

Hada, T., Kennel, C.F. and Buti, B., Stationary Nonlinear Alfvén Waves and solitons, *J. Geophys. Res.,94*, 65, 1989.

Hada, T., Kennel, C.F., Buti, B. and Mjolhus, E., Chaos in Driven Alfvén systems, *Phys. Fluids, B2*, 2581, 1990.

Jatenco-Pereira, V., Alfvén Waves in Astrophysical Plasmas, *Physica Scripta, T60*, 113, 1995.

Karney, C.F.F., Stochastic Ion Heating by a Lower Hybrid Wave, *Phys. Fluids, 21*, 1584, 1978.

Karney, C.F.F. and Bers, A., Stochastic Ion Heating by a perpendicularly propagating Electrostatic Wave, *Phys. Rev. Lett., 39*, 550, 1977.

Kaup, D.J., and Newell, A.C., An exact Solution for a Derivative Nonlinear Schrödinger Equation, *J. Math. Phys., 19*, 798, 1978.

Kennel, C. F., Buti, B., Hada, T. and Pellat, R., Nonlinear, Dispersive, Elliptically Polarized Alfvén Waves, *Phys. Fluids, 31*, 1949, 1988.

Kraichnan, R.H., Inertial Range Spectrum of Hydromagnetic Turbulence, *Phys. Fluids, 8*, 1385, 1965.

Lakhina, G.S. and Buti, B., Coherent Radiation Mechanism for Cometary Kilometric Radiation, *Astrophys. J., 327*, 1020, 1988.

Lakhina, G.S. and Buti, B., Stochastic Acceleration by Lower Hybrid Waves in the Solar Corona, *Solar Phys., 165*, 329, 1996.

Lakhina, G.S., Buti, B. and Tsinsadze, N.L., Radiation from Accelerated Alfvén Solitons in Inhomogeneous Plasmas, *Astrophys. J., 352*, 747, 1990.

Marsch, E. & Liu, S., Structure Functions and Intermittency of Velocity Fluctuations in the Inner Solar Wind, *Ann. Geophys.,11*, 227, 1993.

Medvedev, M.V. and Diamond, P.H., Fluid Models for Kinetic Effects on Coherent Nonlinear Alfvén Waves. I. Fundamental Theory, *Phys. Plasmas, 3*, 863, 1996.

Mjolhus, E. and Wyller, J., Alfvén Solitons, *Physica Scripta, 33*, 442, 1986.

Mjolhus, E. and Wyller, J., Nonlinear Alfvén Waves in a Finite - Beta Plasma, *J. Plasma Phys., 40*, 299, 1988.

Mohan, M. and Buti, B., Modulated Ion Acoustic Waves in Inhomogeneous Plasmas, *Plasma Phys., 21*, 713, 1979.

Nocera, N. and Buti, B., Low Dimensional Structures in Numerical Simulations of DNLSE, *Proc.94ICPP,* edited by P.H. Sakanaka et al., p 115, INPE, Sao Jose dos Campos, SP, Brazil, 1995.

Nocera, L. and Buti, B., Acceleration of Alfvén solitons, *Physica Scripta, T63*, 186, 1996.

Nocera, N. and Buti, B., Bifurcations of Coherent States of the DNLS Equation, in *New Perspectives in the Physics of Mesoscopic Systems, ed. S. De Martino et al., World Scientific, Singapore*, 225, 1997.

Nocera, L. and Buti, B., Organization in the DNLS Equation, *Cont. Fusion and Plasma Phys.,22C*, 2295, 1998.

Ott, E., Grebogi, C. and York, J.A., Controlling Chaos, *Phys. Rev. Lett., 64*, 1196, 1990.

Pettini, M., Nocera, L., & Vulpiani, A., Compressible MHD Turbulence: An

Efficient Mechanism to Heat Stellar Coronae, in *Chaos in Astrophysics, ed. J.R. Buchler et al., Dordrecht: Reidel*, 305, 1985.

Rogister, A., Parallel Propagation of Nonlinear Low-Frequency Waves in High β Plasma, *Phys. Fluids 14*, 2733, 1971.

Roychoudhury, A., Buti, B. and Dasgupta, B., Large amplitude Alfvén soliton in solar wind and Painléve analysis, *Australian J. Phys., 51*, 125, 1997.

Sato, T. and the Complexity Simulation Group, Complexity in Plasma: From Self-organization to Geodynamo, *Phys. Plasmas, 3*, 2135, 1996.

Scarf, F. L., Coroniti, F. V., Kennel, C. F., Gurnett, D. A. and Smith, E. J., Plasma wave observations at Comet Giacobini-Zinner, *Science, 232*, 377, 1986.

Smith, G.R. and Kaufman, A.N., Stochastic Acceleration by a Single Wave in a Magnetic Wave Field, *Phys. Rev. Lett., 34*, 1613. 1975.

Spangler, S.R., Kinetic Effects of Alfvén Wave Nonlinearity. I. Pondermotive Density Fluctuations, *Phys. Fluids, B1*, 1738, 1989.

Spangler, S.R., Kinetic Effects of Alfvén Wave Nonlinearity. II. The Modified Nonlinear Wave Equation, *Phys. Fluids, B2*, 407, 1990.

Spangler, S. R., The Dissipation of Magnetohydrodynamic Turbulence Responsible for Interstellar Scintillation and the Heating of the Interstellar Medium, *Astrophys.J., 376*, 540, 1991.

Tanuiti, T., and Wei, C.C., Reductive Perturbation Method in Nonlinear Wave Propagation. I, *J. Phys. Soc. Japan, 24*, 941, 1968.

Tsurutani, B. T. and Smith, E.J., Strong Hydromagnetic Turbulence associated with comet Ziacobini-Zinner, *Geophys. Res. Lett. 13*, 259, 1986.

Tu, C.Y., & Marsch, E., MHD Structures, Waves and Turbulence in the Solar Wind: Observations and Theories, *Space Sci. Rev., 73*, 1, 1995.

Verheest, F. and Buti, B., Parallel Solitary Alfvén Waves in Warm Multispecies Beam-Plasma Systems *J. Plasma Phys., 47*, 15, 1992.

Verheest, F. and Meuris, P., Nonlinear Electromagnetic Modes in Plasmas with Variable Dust Charges, *Phys. Lett., 210A*, 198, 1996.

Velli, M., Buti, B., Goldstein, B.E. and Grappin, R., Propagation and Disruption of Alfvénic solitons in the Expanding Solar Wind in *Solar Wind Nine, AIP Proceedings,471*, Eds. S. Habbal et al., p. 445, American Institute of Physics, 1999.

Zakharov, V.E., Collapse and Self-Focusing of Langmuir Waves, in *Handbook of Plasma Physics,* Eds. M.N. Rosenbluth and R.Z. Sagdeev, p 81, Elsevier Science Publisher, 1984.